STEM CELLS / Volume 35, Issue 2

Tissue-Specific Stem Cells

Adipose Stromal Vascular Fraction-Mediated Improvements at Late-Stage Disease in a Murine Model of Multiple Sclerosis

Annie C. Bowles, Amy L. Strong, Rachel M. Wise, Robert C. Thomas, Brittany Y. Gerstein, Maria F. Dutre Ryan S. Hunter, Jeffrey M. Gimble, Bruce A. Bunnell

First published: 12 October 2016
https://doi.org/10.1002/stem.2516
Cited by:3

Authored by a member of IFATS

ABSTRACT

Multiple sclerosis (MS) is a common neurodegenerative disease and remains an unmet clinical challenge. In MS, an autoimmune response leads to immune cell infiltration, inflammation, demyelination, and lesions in central nervous system (CNS) tissues resulti in tremors, fatigue, and progressive loss of motor function. These pathologic hallmarks a effectively reproduced in the murine experimental autoimmune encephalomyelitis (EAE) model. The stromal vascular fraction (SVF) of adipose tissue is composed of adipose-derived stromal/stem cells (ASC), adipocytes, and various leukocytes. The SVF can be culture expanded to generate ASC lines. Clinical trials continue to demonstrate the safety and efficacy of ASC therapies for treating several diseases. However, little is known abou the effectiveness of the SVF for neurodegenerative diseases, such as MS. At late-stage disease, EAE mice show severe motor impairment. The goal for these studies was to test the effectiveness of SVF cells and ASC in EAE mice after the onset of neuropathology. The

more robust improvements to CNS pathology than ASC treatment based on significant modulations of inflammatory factors. The most pronounced changes following SVF treatment were the high levels of interleukin-10 in the peripheral blood, lymphoid and CI tissues along with the induction of regulatory T cells in the lymph nodes which indicate potent immunomodulatory effects. The data indicate SVF cells effectively ameliorated th EAE immunopathogenesis and supports the potential use of SVF for treating MS. STEM CE *2017;35:532–544*

SIGNIFICANCE STATEMENT

The evidence reported in this article is the first to demonstrate the effectiveness of using adipose stromal vascular fraction (SVF) cells as therapy at late-stage disease in a model of multiple sclerosis (MS). SVF is the freshly used product of fat digestion that contains adipose-derived stem cells and several other cell types. It is believed that this combination of cells produces robust anti-inflammatory, immunomodulatory, and regenerative effects in vivo when used as therapy. The results from this study provides compelling evidence that supports the use of SVF cells as therapy in a mouse model of MS.

INTRODUCTION

Multiple sclerosis (MS) is a prevalent neurodegenerative disease caused by an aberrant immune response against integral components of the central nervous system (CNS). Althou most MS patients are diagnosed with the relapsing-remitting form, the majority of patients eventually develop a progressive form of the disease exhibiting severe debilities 1, 2. The experimental model that best represents the progressive forms of MS is called the chronic experimental autoimmune encephalomyelitis (EAE) model resulting in comparable patholog features in the CNS 3, 4. In both MS and EAE, autoreactive immune cells including T and B lymphocytes, are primed to destroy myelin resulting in the breakdown of the blood-brain barrier (BBB), infiltration of immune cells into CNS tissues, and generation of inflammatory and demyelinating lesions 2-4.

Adipose is a readily accessible tissue containing a high yield of cells 5, 6. Harvested adipose

stromal/stem cells (ASC), adipocytes, endothelial cells, smooth muscle cells, and several type of leukocytes 5, 7-9. By ex vivo culture expansion, ASC were isolated and discovered as the multipotent cells within adipose 5, 8, 10, 11. By expression of distinct transmembrane receptors, including integrin α4β1, ASC are capable of migration across the BBB to home to local areas of CNS pathology and potentially exert neuroregenerative, immunomodulatory, and anti-inflammatory effects 12. In a model of Parkinson's disease, ASC transplantation has been found to promote neurogenesis and improve motor function demonstrating their therapeutic efficacy for neurodegenerative diseases 11. In vitro, ASC support the survival an differentiation of neural stem cells suggesting therapeutic effects that promote repair and neural plasticity 13. Other studies have demonstrated the immunomodulatory effects of AS by reducing the production of pro-inflammatory cytokines, infiltration of inflammatory cells, and Th1-cell activation 14. By thwarting Th1-mediated autoimmune and inflammatory responses, ASC can induce immune tolerance 15. Moreover, the induction of regulatory T ce following ASC infusion was shown in models of chronic colitis and sepsis 14. These studies demonstrate the efficacy of ASC to comprehensively treat autoimmune diseases by counter inflammation and autoimmune responses and re-establishing immune tolerance 14-16. However, using the SVF for ex vivo culture expansion to isolate ASC involves time, expense, possible biological changes to the cells, and risk of cell contamination and loss 5. The alternative is to investigate the efficacy of fresh SVF cells as a therapeutic substitute for ASC.

The safety and efficacy of using SVF to supplement fat grafts for reconstruction of soft tissue defects have been evaluated in both humans 8, 17 and mice 18 resulting in the safe, enhanc retention, and overall improved quality of the graft without major complications 8, 17, 18. Moreover, the therapeutic use of SVF has been efficacious to veterinary medicine for the treatment of bone, joint, and tendon injuries as well as osteoarthritis in larger animals with adverse effects reported 19-22. Our group previously demonstrated the safety and efficacy SVF as a prophylactic treatment in EAE mice that successfully attenuated the severity of disease 7, 23.

In this study, EAE mice were administered SVF cells, ASC, or vehicle by intraperitoneal (i.p.) injection at 20 days post induction (DPI) of disease, a time point corresponding to severe disease. Improvement to the disease severity, behavior, and motor function in all measured parameters was seen in EAE mice treated with SVF and ASC. Robust modulation of inflammatory mediators in the serum and CNS tissues of both ASC- and SVF-treated EAE mi correlated with the marked improvement in the levels of cell infiltrates, myelin, and lesions. Furthermore, a significantly greater anti-inflammatory milieu and an induction of regulatory cells were revealed in the lymphoid tissues from the SVF-treated EAE mice. These results

comprehensive amelioration of disease amongst all groups. These results provide insight in the mechanistic effects of SVF at late-stage disease and add to the growing body of ongoing research using SVF therapy for neurodegenerative diseases.

Materials and Methods

EAE Induction Using MOG_{35-55} Peptide

Female C57Bl/6 mice (Charles River Laboratories, Wilmington, MA; 6-8 weeks old) were induced with EAE using MOG_{35-55} peptide (AnaSpec, Fremont, CA) as previously described 25. All animal procedures were in compliance and approved by the Institutional Animal Care and Use Committee at Tulane University.

Isolation of the Stromal Vascular Fraction

Inguinal white adipose tissue was collected from enhanced green fluorescence protein transgenic female mice (C57Bl/6-Tg(UBC-GFP)30Scha/J strain; Jackson Laboratory, Bar Harbo ME) between the ages of 6-12 weeks. Adipose was washed 3-4 times with phosphate buffere saline (PBS; Hyclone Laboratories, Inc., Logan, UT), finely minced, and digested with a solutio containing 0.1% (w/v) collagenase type I and 1.0% (w/v) bovine serum albumin (Sigma-Aldric St. Louis, MO) in PBS for 1 hour at 37ºC. Digestion reaction was neutralized with complete culture media (CCM) that contained Dulbecco's Modified Eagle Medium: Nutrient Mixture F- (Thermo Fisher Scientific, Waltham, MA), 10% fetal bovine serum (Atlanta Biologicals, Inc., Flowery Branch, GA), 100 units per mililiter antimycotic/antibiotic and 2 mM L-glutamine (Thermo Fisher Scientific). Digested tissue was filtered, centrifuged, and resuspended in Har balanced salt solution (HBSS; Thermo Fisher Scientific).

Isolation, Expansion, and Characterization of ASC

The SVF was plated in 15 cm^2 culture plates containing CCM, which was incubated at 37ºC w 5% humidified CO_2. After 24 hours, plates were washed of nonadherent cells, and fresh CCM was added to each plate. At 70% confluence, cells were passaged by trypsinization with 0.25 trypsin/1 mM ethylenediaminetetraacetic acid (Gibco, Thermo Fisher Scientific), neutralized with CCM, centrifuged, and re-plated at a low density for culture expansion. This process wa repeated for subsequent passages, and then cells were cryopreserved prior to experimenta use.

For all characterization assays, ASC at passage 3 were used. Adherent ASC were observed fo the spindle-shaped morphology and GFP^+ expression using bright field and fluorescence

Flow cytometric analysis of the cell surface marker profile of ASC was performed. ASC were then labeled with the primary antibodies for anti-mouse: CD106, Sca-1, CD29, CD31, CD11b, CD45, isotype-control IgG1, isotype-control IgG2a, and isotype-control IgG2b (eBioscience, S Diego, CA). The cell surface marker expression of ASC was analyzed on a BD LSRII analyzer (Becton Dickinson, Durham, NC) using Kaluza software (Beckman Coulter, Inc., Brea, CA). AS were analyzed by forward and side scatter of light and at least 5,000 events were acquired a analyzed against isotype-controls.

For differentiation assays, ASC were incubated at 37°C with 5% humidified CO_2 in CCM. At 7(confluence, CCM was replaced with osteogenic or adipogenic differentiation media and fres differentiation media was replaced every 3-4 days 26. After 21 days, cells were fixed in 10% formalin for 1 hour at RT, washed, and stained with 0.5% Oil Red O (Sigma-Aldrich) for 1 hou at RT. Images were acquired at 4× magnification for osteogenic differentiation and 20× magnification for adipogenic differentiation for visualization of bone deposition and lipid vacuoles, respectively, using a Nikon Eclipse TE200 (Melville, NY) with a Nikon Digital Camera DXM1200F using the Nikon ACT-1 software version 2.7.

The growth of ASC was measured using alamarBlue (Thermo Fisher Scientific) cell viability assay at 1, 3, 5, 7, and 9 days after the initial ASC seeding. Using a 48-well culture plate, 2,00 ASC were plated in triplicate for each time point. At each time point, alamarBlue was added each well and incubated at 37°C for 1 hour. The fluorescence intensity of the supernatants were then read at 545 nm excitation and 590 emissions on a plate reader (FLUOstar optima, BMG Labtech, Cary, NC).

Colony forming unit assays were performed in triplicate by seeding 100 cells per 10 cm^2 culture plate. Plates were incubated at 37°C with 5% humidified CO_2 for 14 days, and fresh CCM was replaced every 3-4 days. Plates were washed and stained with 3% crystal violet (Sigma-Aldrich) for 30 minutes at RT then washed and allowed to dry. The number of colonie >2 mm in diameter were counted and reported as the mean ± standard deviation (SD).

Preparation and Injection of Cells

On the days of treatment (20 DPI), cryopreserved ASC were thawed and fresh SVF cells were harvested. Cells were washed with PBS and live cells were counted using a trypan blue exclusion assay on a hemocytometer. Randomly designated mice for treatment were administered either 1×10^6 ASC or SVF cells in 100 µl HBSS, and vehicle control mice were given 100 µl HBSS via i.p. injection.

clinical scoring system used is described as: (0)- no detectable signs; (1)- loss of tail tone with mildly abnormal gait; (2)- hind limb weakness; (3)- partial paralysis of hind limbs; (4)- comple paralysis of hind limbs; (5)-moribund or death. The mean clinical scores were calculated by averaging the clinical score for all mice in each group recorded from 20-30 DPI. The cumulat scores were determined by the summation of all scores reported from 20 DPI to 30 DPI for each mouse per group. Clinical scores, mean scores, and cumulative scores are presented a mean ± SD for the vehicle ($n = 8$), ASC ($n = 6$), and SVF ($n = 8$) treatment groups. For 5, 10, 15, 2 25, and 30 DPI, each mouse was placed in a cylindrical arena, assessed for behavioral performance, and video recorded for a total of 5 minutes. Video recordings were captured with Windows Movie Maker software and analyzed with Ethovision XT7 (Noldus IT, Leesburg VA) for measurement of several parameters as previously described 27. For the behavior an motor function assessments, the vehicle ($n = 5$), ASC ($n = 5$), and SVF ($n = 5$) groups are presented as the mean ± standard error of the mean (SEM).

Tissue Harvest and Processing

At the endpoint (30 DPI, 10 days post cell infusion), mice were euthanized by CO_2 asphyxiati Blood was collected by intracardial puncture for serum extraction or collection of whole blo for flow cytometry analysis. Subsequently, intracardial perfusion with sterile PBS was performed and tissues were collected. Peripheral blood, draining lymph nodes, spleens, brains, and spinal cords were harvested. The volume of peripheral blood and the weights of lymph nodes and spleens were documented. Cervical spinal cord sections were placed in 1(phosphate buffered formalin (Newcomer Supply, Inc.) for histology, and the remaining spina cord was purged from the vertebral column and placed in a collection tube for RNA isolatior Peripheral blood mononuclear cells (PBMC) were collected from the buffy coats obtained by density gradient centrifugation of whole blood using Ficoll-Paque PREMIUM (GE Healthcare, Thermo Fisher Scientific), washed, and then stored at −80°C. Sera and tissues samples designated for RNA isolation were stored in −80°C. The brain and spinal cord were collected together and mechanically digested with a 15 ml Dounce homogenizer. Mononuclear cells o the CNS tissues were isolated by density gradient centrifugation. Briefly, homogenized CNS tissue was prepared in 30% Ficoll solution that was carefully overlayed on a 70% Ficoll soluti and centrifuged at 500*g* for 30 minutes at 18°C. Cells of the CNS were collected at the 30%/7 interphase, washed, and immediately processed for flow cytometric staining.

Flow Cytometric Staining and Analysis

Spleens and lymph nodes were homogenized into single-cell suspensions by mechanical

7.2-7.4, Sigma-Aldrich) for 5 minutes. Cells obtained from the CNS, lymph node, spleen, and blood were counted, prepared in blocking solution and labeled with extracellular anti-mous antibodies: CD3e-PE-eFluor 610 CD4-PE, CD8-PE-Cy5, CD25-APC-eFluor 780, CD45-Alexa Fluo 700, CD19-PE-eFluor 610, F4/80-APC-eFluor 780, FcεR1-PE-Cy7, and Ly6G-APC-eFluor 780 (eBioscience, San Diego, CA) as previously described 25. Samples for intracellular staining w incubated with Fixation/Permeabilization Concentrate and Diluent (eBioscience) according t manufacturer's instructions then stained with anti-mouse rat Foxp3-eFluor 660 (eBioscience for 30 minutes at RT in the dark and washed twice with 1× Permeabilization Buffer (eBioscience). All samples were stored at 4°C prior to flow cytometric analysis using a BD LS analyzer (Becton Dickinson), and Kaluza 1.2 software (Beckman Coulter) was used for data acquisition of at least 2,500 events per sample.

Histological Analyses

Cervical spinal cord sections were processed and stained with hematoxylin and eosin (H&E; Richard-Allan Scientific, Thermo Fisher Scientific) and Luxol fast blue (IHC World, LLC, Woodstock, MD) and analyzed for quantitative comparison as previously described 24. H&E-stained sections were used for quantification of lesion frequency and surface area which we detected by areas of high cellularity near the perivasculature.

Briefly, immunohistochemistry was performed on paraffin-embedded spinal cord sections b deparaffinization, rehydration, and heat-mediated antigen retrieval method. Next, sections were blocked and incubated overnight at 4°C in the dark with primary antibodies: rabbit ant mouse CD3, CD4 (Abcam), CD19 (eBioscience), and F4/80 (Invitrogen). Sections were washed and incubated for 1 hour at RT in the dark with goat anti-rabbit IgG conjugated to Alexa Fluo 594 (Invitrogen) then mounted with ProLong Gold antifade reagent with 4′,6-diamidine-2'-phenylindole dihydrochloride (Thermo Fisher Scientific). Images were taken at 20× magnification using a Nikon Eclipse E800 (Nikon, Melville, NY) microscope and acquired with Slidebook version 5.0 software (Olympus, Center Valley, PA).

RNA Isolation, cDNA Generation, and Quantitative Real-Time RT-PC

Qiazol Tissue Protectant (Qiagen, Valencia, CA) was added to thawed tissue samples and homogenized with a motorized pellet pestle and tip (Kimble Chase, Vineland, NJ). For total R extraction, each sample was processed using RNeasy Mini Kit (Qiagen) according to the manufacturer's instructions. RNA was subsequently purified with DNase I (Invitrogen) and reverse transcribed using the SuperScript VILO cDNA synthesis kit (Invitrogen). Mouse-speci primers were generated for gene expression analysis of transforming growth factor-β (TGF-

(Supporting Information 5). EXPRESS SYBR GreenER qPCR SuperMix Kit (Invitrogen) was used for quantitative real-time RT-PCR (qPCR) according to manufacturer's instructions and ΔΔCt was calculated to quantify mRNA expression levels.

Cytokine Detection

Serum samples were thawed at RT. Equal volumes of sera from 6 individual mice within the same group were pooled, and cytokines levels were measured using a Mouse Inflammatory Cytokines Multi-Analyte ELISArray Kit (Qiagen), according to the manufacturer's instructions. Briefly, pooled sera were incubated in the wells of 96-well precoated plates at RT. Wells were incubated with a detection antibody, secondary antibody, and development solution then a stop solution was added. The plates were then read with at OD450 on a fluorescent micropl reader (FLUOstar optima). For each cytokine, the absorbance values for each group's sample was standardized by subtraction of the appropriate negative control then divided by the val of the positive control and presented as the normalized absorbance ratio (NAR).

Statistical Analysis

Statistical analysis of the single measurable parameters was performed using one-way analy of variance (ANOVA) followed by pairwise comparisons of the mouse groups using Bonferro post hoc testing. For the flow cytometric and qPCR analyses, statistical analysis of all groups was performed using two-way ANOVA followed by the pairwise Bonferroni post hoc testing. Significance for individual pairwise comparisons and the overall group effect was defined as $< .05$. Analysis was performed using Prism 5.0 (Graphpad Software, La Jolla, CA).

RESULTS

Characterization of Mouse SVF and ASC

The populations of cells within the SVF were classified by the cell marker expressions system (Supporting Information 1) and expressed as the frequency, or percent of total events (% tot collected by flow cytometry. The majority of cells that compose the SVF are $CD34^+$ cells, the lymphohematopoietic population (12.48 ± 0.75% total) and ASC (9.93 ± 0.63% total). Other ce types detected in the SVF included adipocytes (6.43 ± 0.71% total), endothelial cells (2.61 ± 0.32% total), and smooth muscle cells (4.43 ± 0.32% total). Of the myeloid lineage, the granulocytes, mast cells, and macrophages made up 5.50 ± 0.87%, 4.38 ± 0.46%, and 4.26 ± 0.38% total, respectively. $CD3^+$ expression measured all T cells (7.57 ± 1.14% total) which included the cytotoxic T cells (5.17 ± 0.56% total) and other subsets, the helper T cells and

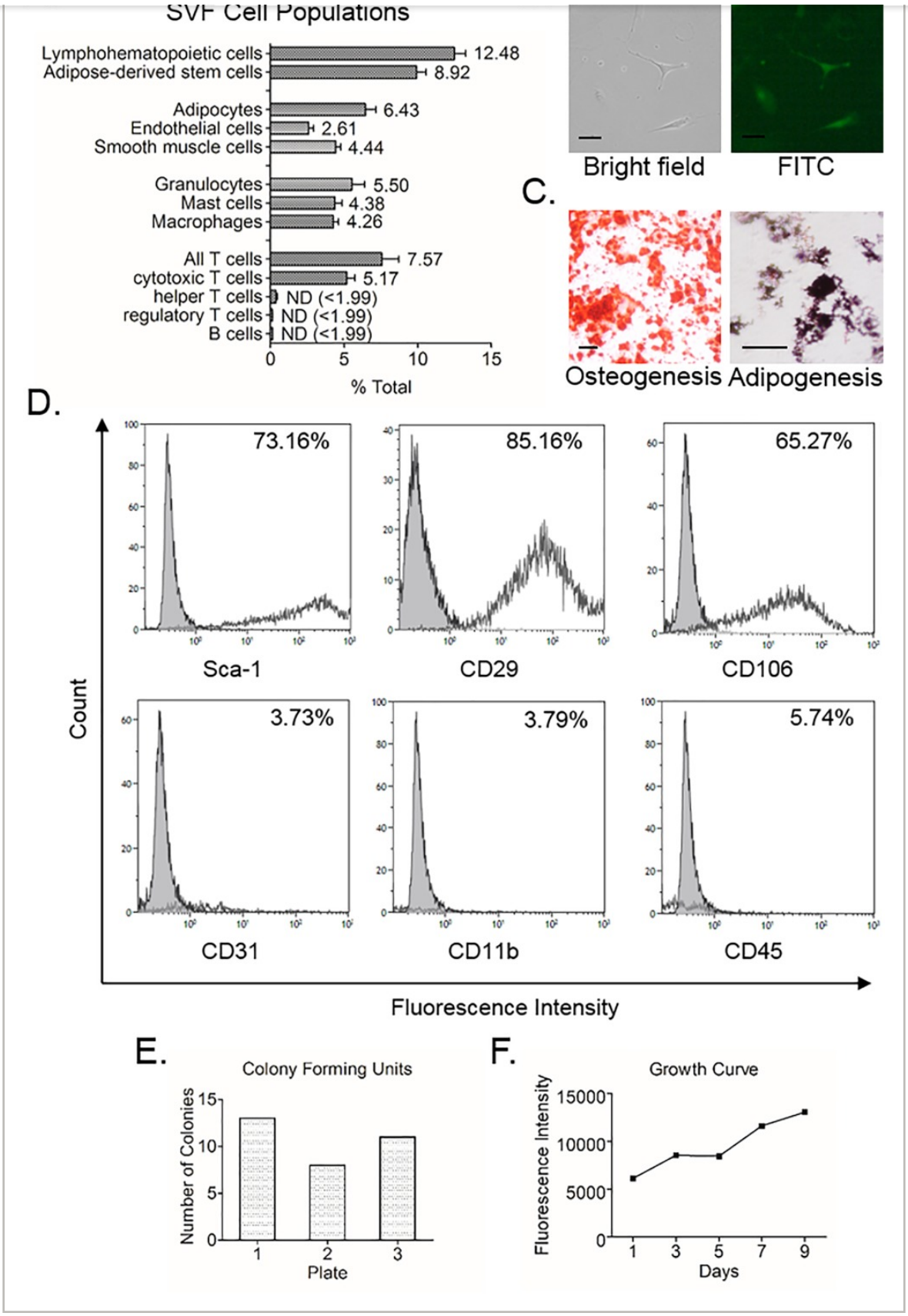
SVF Cell Populations
Lymphohematopoietic cells 12.48
Adipose-derived stem cells 8.92
Adipocytes 6.43
Endothelial cells 2.61
Smooth muscle cells 4.44
Granulocytes 5.50
Mast cells 4.38
Macrophages 4.26
All T cells 7.57
cytotoxic T cells 5.17
helper T cells ND (<1.99)
regulatory T cells ND (<1.99)
B cells ND (<1.99)
0 5 10 15
% Total
Bright field
FITC
C.
Osteogenesis
Adipogenesis
D.
73.16%
85.16%
65.27%
Sca-1
CD29
CD106
3.73%
3.79%
5.74%
CD31
CD11b
CD45
Count
Fluorescence Intensity
E.
Colony Forming Units
Number of Colonies
Plate
F.
Growth Curve
Fluorescence Intensity
Days

Figure 1

expression of the GFP transgene (Fig. 1D). To assess multipotency, ASC were induced to differentiate into osteogenic and adipogenic lineages. Both osteogenesis and adipogenesis were confirmed by observation of calcium deposition and neutral lipid vacuoles, respectively (Fig. 1C). The cell surface antigen profile of ASC showed high positive expression of Sca-1 (73.16% total), CD29 (85.16% total), and CD106 (65.27% total) and low detection of CD31 (3.7 total), CD11b (3.79% total), and CD45 (5.74% total; Fig. 2D). The ability of ASC to self-renew w demonstrated by the generation of 10.7 ± 2.5 colony forming units (Fig. 2E). To show the growth of ASC over time, the increased fluorescence intensity throughout the designated tir points of 1, 3, 5, 7, and 9 days were detected as the values of 6133, 8545, 8448, 11623, and 13047, respectively (Fig. 2F).

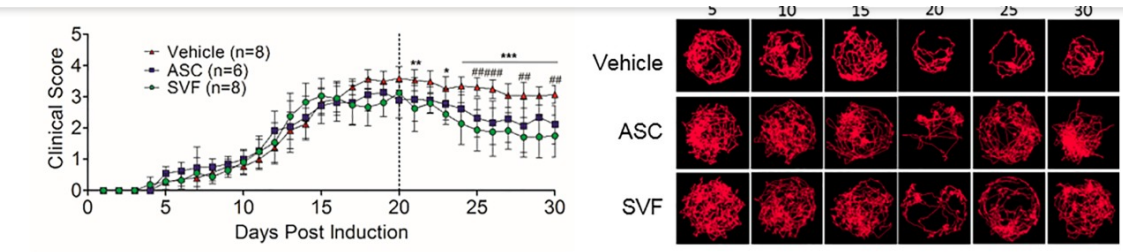

C.

Treatment	Mean score (range)	Cumulative disease score	Unprotected rears (total)	Wall leans	Grooming Bouts
Vehicle	3.3 ± 0.2 (2.5-3.5)	32.9 ± 3.2	0.2 ± 0.4	0.4 ±0.5	2.2 ± 0.8
ASC	2.5 ± 0.3## (0.5-3)	28.1 ± 5.4	7.4 ± 6.1	3.6 ± 1.3##	4.8 ± 4.6
SVF	2.2 ± 0.5*** (1-2.5)	25.3 ± 1.6**	9.0 ± 6.4	5.0 ± 1.6***	1.8 ± 0.4

Figure 2

Open in figure viewer | PowerPoint

SVF and ASC therapies mediated functional improvements at late-stage EAE disease. **(A)**: The amelioration of the disease severity was demonstrated by significant reductions in daily clinical scoring after treatment at 20 DPI in both the SVF- and ASC-treated EAE groups compared to the vehicle-treated EAE group. Mean ± SD. **(B)**: Visuals of the compiled tracks of a representative mouse recorded in a cylindrical arena for 5 minutes every 5 days during the course of disease show increased tracked area depicted in the SVF and ASC treatment groups compared to the Vehicle group. **(C)**: Quantitative comparisons of the mean scores and cumulative disease scores from 20 DPI (injection date) to 30 DPI to correlate the effects of each treatment and reduction of the severity of disease. Additionally, SVF- and ASC-treated EAE mice show increased execution of multiple behaviors at 30 DPI compared to vehicle-treated EAE mice ($n = 5$). Mean ± SD. *SVF versus vehicle; #ASC versus vehicle; *,# ($p < .05$); **,## ($p < .01$); ***,### ($p < .001$). Abbreviations: ASC, adipose-derived stem cells; SVF, stromal vascular fraction; EAE, experimental autoimmune encephalomyelitis; DPI, days post induction.

Caption

Disease Progression and Neuromotor Activity

recorded for the vehicle (3.0 ± 0.4), ASC (2.9 ± 0.6), and SVF (3.1 ± 0.3), and there was no statistically significant difference between each group. By 30 DPI, a marked reduction in the scores corresponded to diminished disease severity in the ASC (2.1 ± 0.6, $p < .001$) and more the SVF (1.8 ± 0.7, $p < .001$) treatment groups compared to the vehicle (3.1 ± 0.3) control grou (Fig. 2A). Track visuals of a representative mouse from each group over time showed similar deficits of tracked course by 20 DPI (treatment day) which was restored in the ASC- and SVF-treated mice by 5 days after treatment (25 DPI; Fig. 2B). The mean clinical scores of mice treated with ASC (2.5 ± 0.3; $p < .01$) and SVF (2.2 ± 0.5; $p < .001$) were significantly less than th vehicle control group (3.3 ± 0.2). As for the cumulative disease scores, the ASC and SVF treatment groups were quantified as 28.01 ± 5.4 and 25.3 ± 1.6 ($p < .01$), respectively, wherea the score for the vehicle control group was 32.9 ± 3.2 (Fig. 2C). Overall on 30 DPI, the SVF-treated mice showed the most improvement with mice displaying either a score of 1 or 2, whereas the majority of ASC-treated mice displayed a score of 2 and vehicle-treated mice maintained a score of 3 (Supporting Information 2A).

The analysis of behavior demonstrated the extent of each mouse's balance, coordination, a hind limb strength. The vehicle-treated EAE mice were unable to execute any of the observe behaviors at 20 DPI and thereafter. In contrast, the SVF- and ASC-treated EAE mice were abl to perform 1.8 ± 0.6 and 5.4 ± 1.5 wall leans at 25 DPI and 5.0 ± 0.7 and 3.6 ± 0.6 wall leans on DPI, respectively. The unprotected rears performed by SVF- and ASC-treated EAE mice were 4.0 ± 1.0 and 17.8 ± 5.4 at 25 DPI and 9.0 ± 2.9 and 7.4 ± 2.7 at 30 DPI, respectively (Supporting Information 2B). The following data are of motor function parameters measured at 30 DPI. T total distance traveled for the 5 minute duration was markedly increased in the SVF-treated (405.5 ± 44.0 cm) and ASC-treated (572.2 ± 31.3 cm; $p < .05$) EAE mice compared to vehicle-treated (355.6 ± 41.0 cm) EAE mice. The average moving durations of SVF-, ASC-, and vehicle-treated EAE mice were 16.4 ± 1.4 seconds ($p < .05$), 22.2 ± 0.9 seconds ($p < .001$), and 10.9 ± 0. seconds per minute, respectively. Compared to the vehicle control group (1.2 ± 0.07 cm/s), th average velocities of the SVF-treated (1.4 ± 0.09 cm/s) and ASC-treated (2.3 ± 0.12 cm/s; $p < .0$ EAE mice were markedly increased. For the nonmoving duration, the ASC treatment group (38.1 ± 0.9 s; $P < .05$) was greatly reduced compared to the SVF (45.9 ± 1.2 s) and vehicle (49.1 0.9 s) treatment groups (Supporting Information 2C).

Improvements in Spinal Cord Histopathology

Histology of spinal cord sections assessed the pathologic features including the levels of cellular infiltrates, myelin, and lesions. The infiltration of cells was greatly reduced in the spi cords of ASC (118.0 ± 7.2 cells; $p < .001$) and SVF (140.8 ± 13.3 cells; $p < .05$) treatment groups

SVF (92.9 ± 0.7%, $p < .001$) treatment compared to the vehicle group (81.3 ± 1.4%; Figs. 3B, 3F). Lesions were analyzed for their size, or surface area, and frequency (Fig. 3C). Treatment with ASC (5806.9 ± 723.4 μm^2; $p < .05$) and SVF (7110.5 ± 1177.0 μm^2) diminished the size of the lesions compared to the vehicle group (10919.2 ± 1756.5 μm^2; Fig. 3G). Similarly, the frequency of lesions was greatly reduced in the spinal cords of ASC-treated (0.6 ± 0.1 lesions; $p < .001$) and SVF-treated (0.9 ± 0.2 lesions; $p < .001$) EAE mice compared to the vehicle-treated EAE mice (3 ± 0.3 lesions; Fig. 3H).

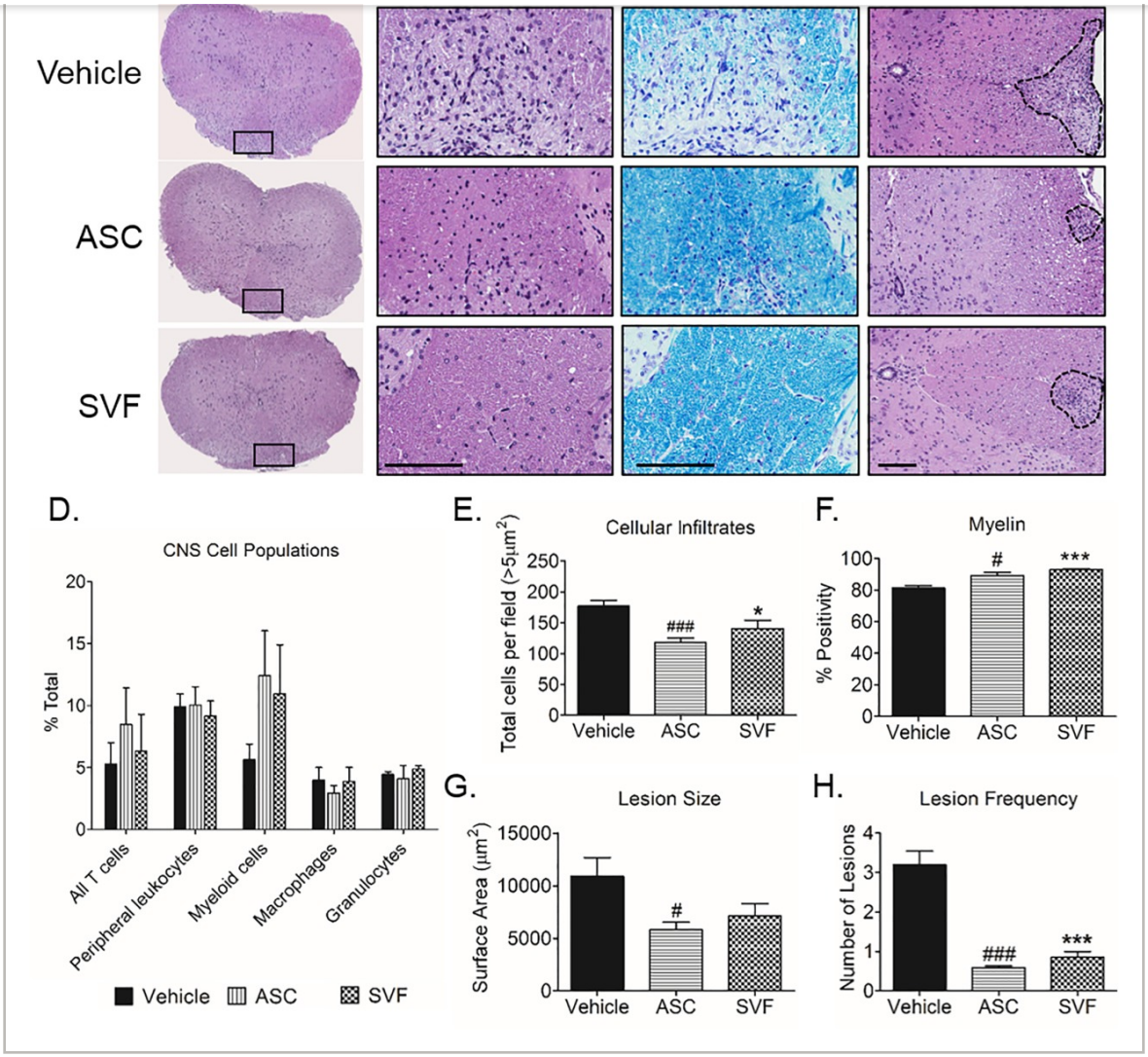

Figure 3

Open in figure viewer | PowerPoint

Histologic analysis of spinal cord pathology after treatment. **(A-C)**: Images of spinal cord sections from vehicle-, ASC-, and SVF-treated EAE mice. Sections were stained with hematoxylin and eosin (H&E) and Luxol fast blue to detect cellular infiltrates and myelin, respectively, and delineations of lesions was executed with H&E-stained sections. Scale bars represent 100 μm. **(D)**: Cell populations isolated from the CNS tissues of mice in each group ($n = 3$) were analyzed using flow cytometry and represented as the mean ± SEM. **(E)**: Quantitative comparison of the levels of cellular infiltration within the spinal cords sections from EAE mice treated with vehicle, ASC, or SVF ($n = 5$). **(F)**: Myelin levels were quantified to compare between vehicle-, ASC-, and SVF-treated EAE groups ($n = 5$). **(G, H)**: Analysis of lesion frequency and surface area

frequencies of $CD3^+$ T cells measured in the vehicle-treated (5.5 ± 1.7% total), ASC-treated (6.3 ± 3.0% total), and SVF-treated (6.3 ± 3.0% total) were comparable. Of the peripheral leukocytes ($CD45^+$ cells), similar frequencies were detected in the vehicle (9.9 ± 1.1% total) and ASC (10.1 ± 1.5% total) treatment groups, whereas a mild reduction was seen in the SVF treatment group (9.1 ± 1.2% total). Both ASC and SVF treatments enhanced the myeloid cells ($CD11b^+$ cells) present in the CNS with frequencies of 12.4 ± 3.6% total and 11.0 ± 4.0% total, respectively, compared to the vehicle treatment (5.6 ± 1.3% total). Together, the macrophages ($F4/80^+$ cells) from the periphery and resident to the CNS were measure which revealed a modest decrease in the ASC-treated group (2.9 ± 0.6% total) compared to the vehicle-treated (4.0 ± 1.0% total) and SVF-treated (3.9 ± 1.1% total) groups. The frequencies of granulocytes ($Fc\varepsilon RI^+$ cells) were comparable in the vehicle (4.4 ± 0.2% total), ASC (4.1 ± 1.1% total) and SVF (4.9 ± 0.3% total) treatment groups (Fig. 3D).

Additionally, immunohistochemical analysis verified that the levels of macrophages and CD3 T cells in the spinal cords amongst all groups were comparable. Analysis of phenotypes for both the helper T cells and B cells in the spinal cords determined an absence of these cell types in the SVF-treated group compared to the other groups. The relative presence of the lymphocytes disseminated throughout the spinal cord tissue sections, although the macrophages were present at higher levels in the perivascular locations (Supporting Information 3).

Robust Induction of Immunomodulatory Cytokines with SVF Treatment in the CNS Tissues

Indications of the disease milieu was provided by the gene expression levels of cytokines in the CNS tissues 10 days after treatment. Overall, SVF treatment induced the greatest change in both the brain and spinal cord. The levels of IL-10 and IL-6 in the spinal cords of SVF-treat EAE mice were 1.9 ± 0.4-fold ($p < .001$) and 13.0 ± 5.8-fold ($p < .001$) higher, respectively, than the vehicle group. Similarly, the levels of IL-10 in the brains of ASC-treated (1.6 ± 0.1; $p < .05$) and SVF-treated (2.1 ± 0.4-fold; $p < .01$) EAE mice compared to the levels in the vehicle-treate group (1.0 ± 0.1-fold). In the spinal cords, SVF treatment increased the levels of TGF-β, TNF-α and IFN-γ to 1.6 ± 0.5-fold ($p < .01$), 2.5 ± 0.8-fold ($p < .001$), and 4.5 ± 1.1-fold ($p < .001$) higher, respectively, than the vehicle group. A marked reduction in the TSG-6 was seen in the spinal cords following SVF treatment (0.7 ± 0.2-fold; $p < .05$) compared to vehicle treatment (Fig. 4).

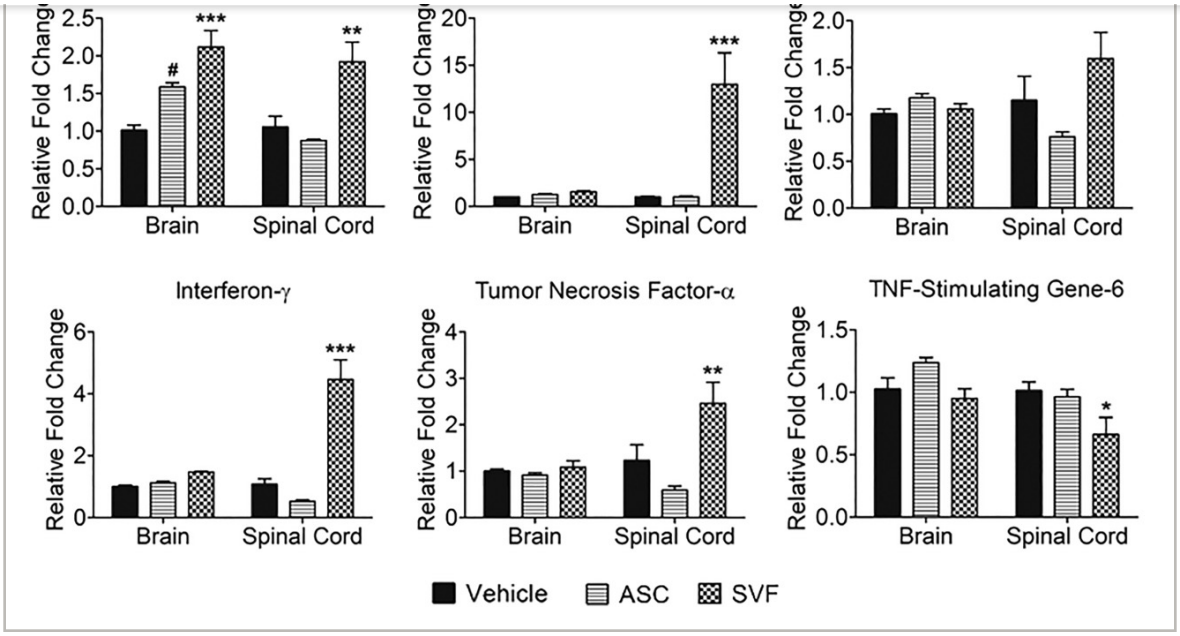

Figure 4

Open in figure viewer | PowerPoint

Gene expression analysis of inflammatory mediators measured in the CNS tissues of treated EAE mice. Analysis of cytokine levels within the brains and spinal cords of ASC- and SVF-treated EAE mice relative to the vehicle-treated EAE mice were detected 10 days after treatment ($n = 3$ for all groups). Data was normalized to the vehicle (=1) and represented as the relative fold change ± SEM. *SVF versus vehicle; #ASC versus vehicle; *,# ($p < .05$); **,## ($p < .01$); ***,### ($p < .001$). Abbreviations: CNS, central nervous system; EAE, experimental autoimmune encephalomyelitis; ASC, adipose-derived stem cells; SVF, stromal vascular fraction.

Caption

SVF Treatment Modulates Immune Cell Frequencies in the Periphe Lymphoid Organs and Blood of EAE Mice

Treatment with SVF demonstrated the greatest alterations to the frequencies of immune ce within the spleens, lymph nodes, and peripheral blood 10 days after treatment. Of the lymphoid populations within the spleens of EAE mice, significantly higher frequencies of all cells (10.0 ± 0.3% total; $p < .001$), helper T cells (6.9 ± 0.5% total; $p < .001$), and B cells (11.1 ± 0.

lineages, the frequency of macrophages showed the largest increase with SVF treatment (54 ± 0.8% total; $p < .001$) compared to treatment with vehicle (5.8 ± 1.2% total) and ASC (4.5 ± 0.2 total) treatment (Fig. 5A). SVF treatment also reduced the frequency of granulocytes to undetectable levels compared to the vehicle (13 ± 2.3% total) and ASC (18.0 ± 7.3% total) treatment. The enlargement of spleens from EAE mice was recorded as 150.3 ± 16.4 mg, 114 ± 13.4 mg, and 146.0 ± 18.8 mg for the vehicle-treated, ASC-treated, and SVF-treated groups, respectively, with an average of $7.5 \pm 1.1 \times 10^5$ cells per milligram splenic tissue (Supporting Information 4).

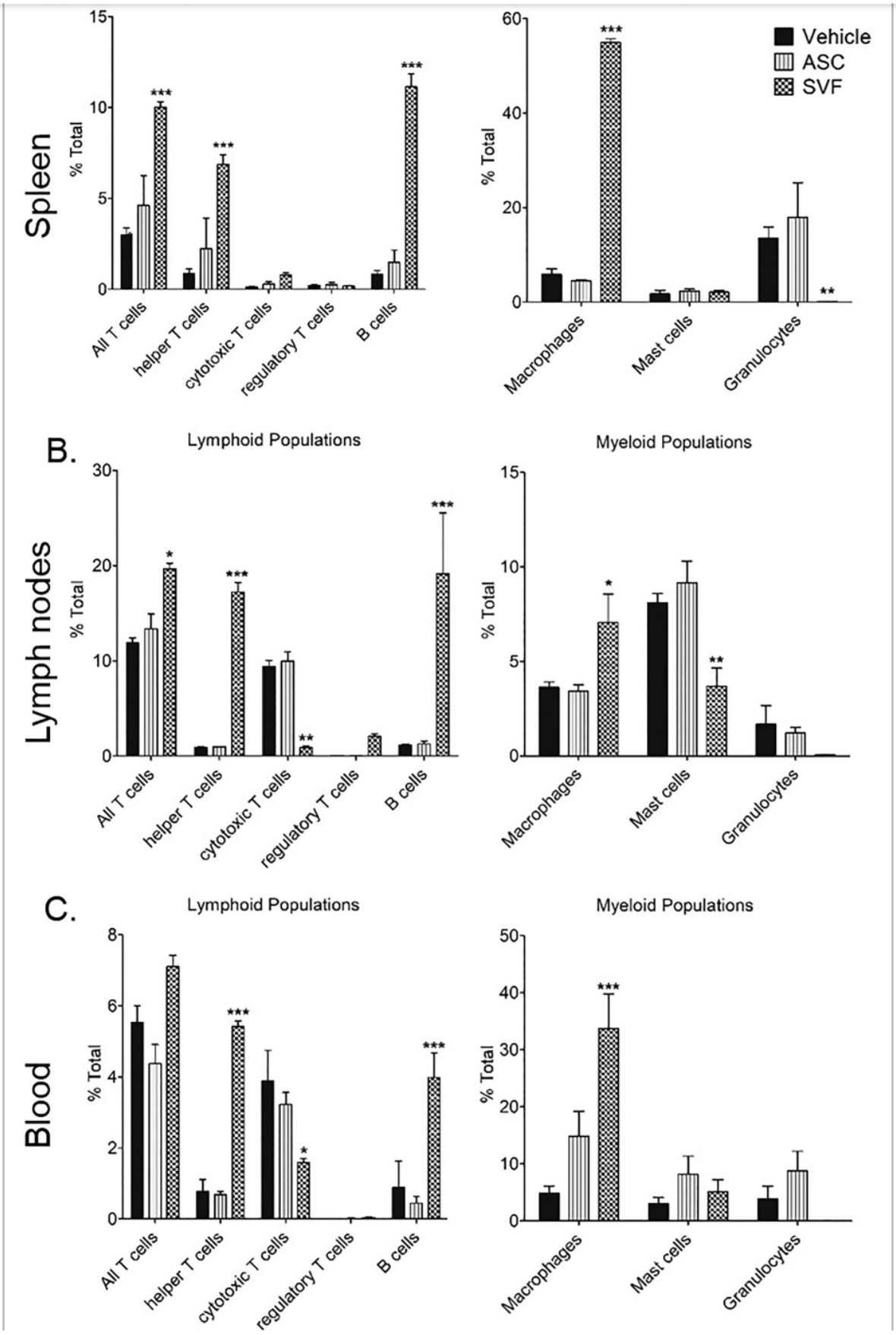
Spleen
% Total
All T cells
helper T cells
cytotoxic T cells
regulatory T cells
B cells
Macrophages
Mast cells
Granulocytes
Vehicle
ASC
SVF
B.
Lymph nodes
Lymphoid Populations
Myeloid Populations
C.
Blood

average of 2.2 ± 0.3 x 10⁴ cells per mg tissue (Supporting Information 4). At the time of harve the lymph nodes of SVF-treated EAE mice contained greater frequencies of all T cells (19.7 ± 0.6% total; $p < .05$), helper T cells (17.2 ± 1.0% total; $p < .001$), and B cells (19.1 ± 6.4% total $p <$ .001) along with a significant decrease in cytotoxic T cells to undetectable levels compared t the vehicle (9.4 ± 0.6% total) and ASC (9.9 ± 1.0% total) treatment groups. Most notably, the regulatory T cells were induced to measurable levels within the lymph nodes of SVF-treated EAE mice (2.1 ± 0.3% total), whereas the regulatory T cells were not detected in either the vehicle-treated and ASC-treated mice. For the myeloid cells, SVF treatment enhanced the frequency of macrophages (7.1 ± 1.5% total; $p < .05\%$) while diminished the frequencies of m cells (3.7 ± 1.0% total; $p < .01$) and granulocytes (undetectable; Fig. 5B).

Similar trends were seen in the cell frequencies within the peripheral blood as the lymph nodes and spleens at 10 days following SVF treatment. The frequencies of all T cells (7.1 ± 0.3 total), helper T cells (5.4 ± 0.2% total; $p < .001$), and B cells (4.0 ± 0.7% total; $p < .001$) were enhanced in the circulating blood of SVF-treated animals. Furthermore, SVF treatment resul in a decreased frequency of cytotoxic T cells to 1.6 ± 0.1% total ($p < .05\%$) compared to the blood from ASC-treated (3.2 ± 0.3% total) and vehicle-treated (3.9 ± 0.9% total) EAE mice. Consistent to the other lymphoid organs, SVF treatment (33.7 ± 6.1% total; $p < .001$) induced large increase in the macrophage frequency compared to ASC (14.9 ± 4.4% total) and vehicle (4.9 ± 1.2% total) treatment groups (Fig. 5C). Together, granulocytes were undetectable in the spleens, lymph nodes, and peripheral blood following SVF treatment (Fig. 4A-4C). From each mouse, an average volume of 290.5 ± 78.5 μl of peripheral blood was collected with a concentration of 1.5 ± 0.1 x 10^4 cells per microliter (Supporting Information 4).

Alterations to Cytokines that Modulate the Phenotypes of Helper T-Cell Subsets and Macrophages in the Lymphoid Organs and Peripheral Blood

To understand the roles of immune cells present in the spleens, lymph nodes, and blood following treatment, gene expression levels of several cytokines that are known to influence phenotypic changes of immune cells were analyzed. Spleens showed the greatest changes following ASC and SVF treatment compared to the vehicle group. Of the cytokines known to modulate T cell subsets, TGF-β expression was markedly enhanced after treatment with ASC (2.8 ± 0.6-fold; $p < .01$) and SVF (2.5 ± 0.7-fold; $p < .05$) compared to vehicle (1.1 ± 0.3-fold). IL-1(expression was 1.7 ± 0.4-fold and 3.1 ± 1.2-fold higher in the spleens of ASC- and SVF-treated EAE mice, respectively, than the vehicle-treated group (1.0 ± 0.2-fold). Similarly, the relative expression of IL-4 in splenic tissue showed 2.3 ± 0.1-fold and 2.7 ± 0.2-fold increases in the A

0.4 ± 0.1-fold decrease compared to vehicle treatment (1.1 ± 0.2-fold). The levels of IFN-γ in t spleen were similar in both the vehicle (1.0 ± 0.2-fold) and ASC (0.9 ± 0.5-fold) treatment grou whereas a 2.8 ± 0.8-fold increase was measured following SVF treatment. PBMC in circulatio of SVF-treated EAE mice had a 0.6 ± 0.2-fold decrease of IFN-γ expression compared to PBM from the vehicle (1.0 ± 0.2-fold) and ASC (1.8 ± 1.0-fold) treatment groups. Expression of IL-12 the lymph nodes showed 0.6 ± 0.1-fold and 0.7 ± 0.1-fold reductions in the ASC and SVF treatment groups, respectively, compared to the vehicle group (1.1 ± 0.2-fold). The expressio of IL-12 in the PBMC from vehicle (1.1 ± 0.2-fold) and SVF (1.2 ± 0.2-fold) treatment groups we comparable, whereas ASC treatment (0.6 ± 0.05-fold) diminished IL-12 expression. The splee of ASC- and SVF-treated EAE mice revealed 0.8 ± 0.4-fold and 0.6 ± 0.3-fold reductions of IL-1 expression compared to the spleens from vehicle-treated mice (1.4 ± 0.4-fold). Changes to th levels of IL-17 in the lymph nodes and PBMC were minimal following ASC and SVF treatment (Fig. 6A).

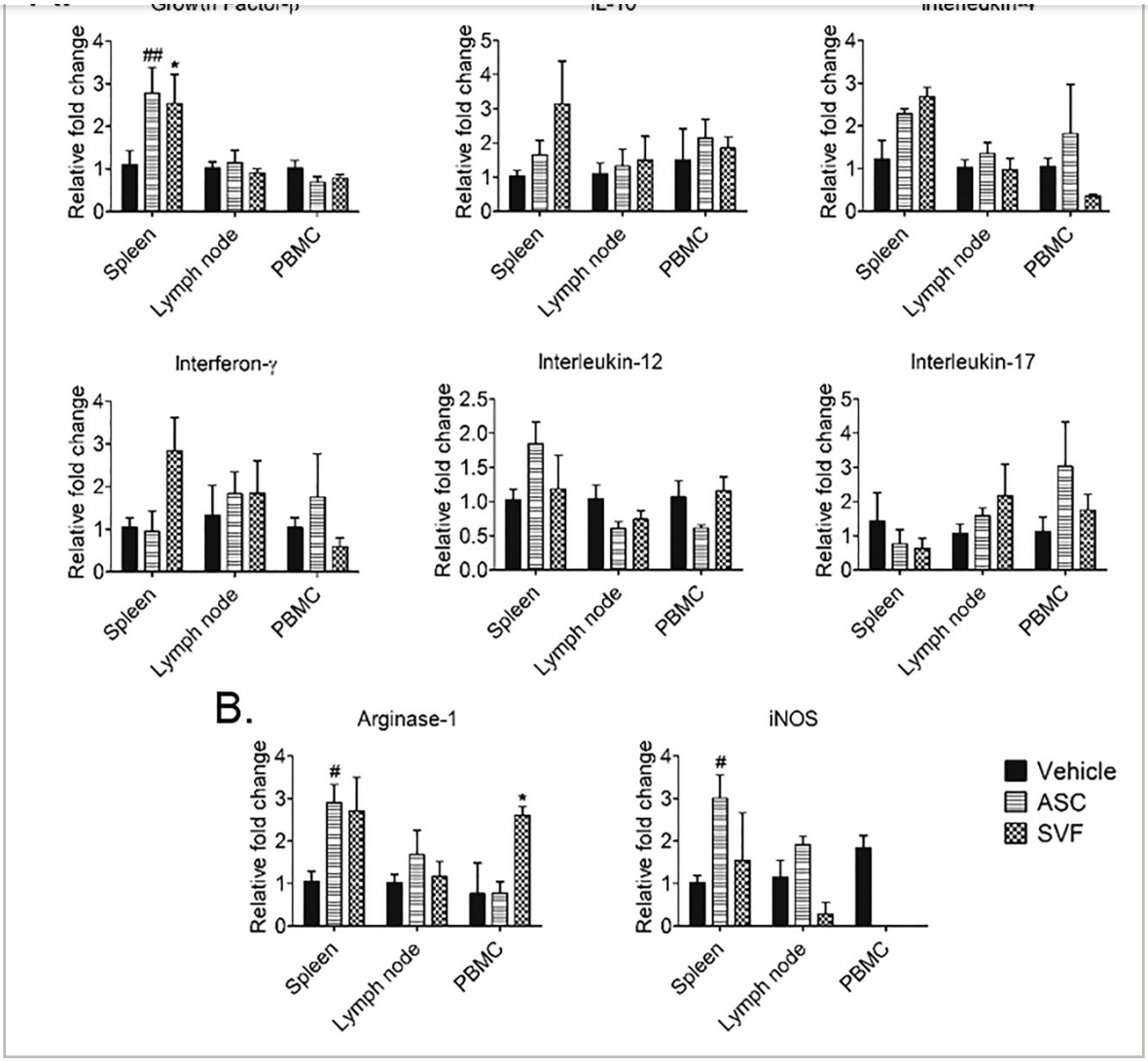

Figure 6

Open in figure viewer | PowerPoint

Alterations of mediators that influence the phenotypic expressions of T cells and macrophages. Cells from the spleen, lymph node, and PBMC of vehicle-, ASC-, or SVF-treated EAE mice were assessed for the gene expressions that correlate with the presence of **(A)** helper T cell subtypes and **(B)** macrophage phenotypes. Mean ± SEM. *SVF versus vehicle; #ASC versus vehicle; *,# ($p < .05$); **,## ($p < .01$); ***,### ($p < .001$). Abbreviations: PBMC, peripheral blood mononuclear cells; ASC, adipose-derived stem cells; SVF, stromal vascular fraction; EAE, experimental autoimmune encephalomyelitis.

Caption

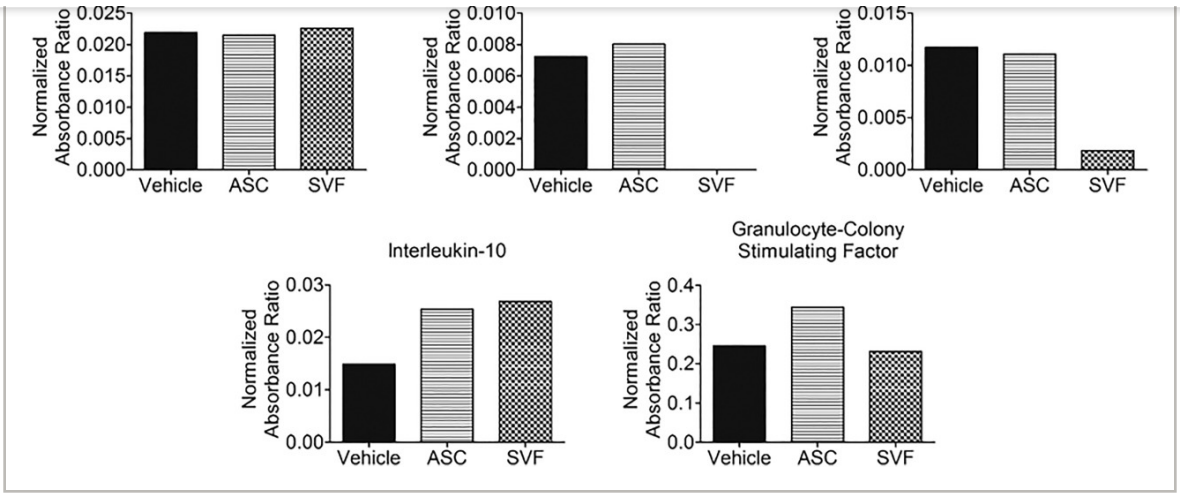

Figure 7

Open in figure viewer | PowerPoint

Serum proteins detected from vehicle-, ASC-, and SVF-treated EAE mice 10 days after administration of therapy at late-stage disease. Quantitative comparison of cytokines in serum samples detected by ELISA from EAE mice treated with Vehicle, ASC, or SVF (six pooled sera samples per group). Data presented as the normalized absorbance ratio. Abbreviations: ASC, adipose-derived stem cells; SVF, stromal vascular fraction; EAE, experimental autoimmune encephalomyelitis.

Caption

The gene expression levels of Arg-1 and iNOS are correlative, yet not exclusive, to the prese of polarized phenotypes of macrophages that indicate alternative activation and classical activation phenotypes, respectively. Arg-1 expression was markedly increased by 2.9 ± 0.4-fc ($p < .05$) and 2.7 ± 0.8-fold in the spleens following ASC and SVF treatment, respectively, than the vehicle treatment group (1.1 ± 0.2-fold). Levels of Arg-1 in PBMC from SVF-treated mice (± 0.2-fold; $p < .05$) was significantly higher than the vehicle-treated mice (0.8 ± 0.7-fold). Although the levels of iNOS were comparable in the spleens of the vehicle and SVF treatmer groups, ASC treatment induced a 3.0 ± 0.5-fold increase. Likewise in the lymph nodes, a 1.9 ± 0.2-fold increase of iNOS was induced with ASC treatment, whereas a 0.3 ± 0.3-fold decrease was measured following SVF treatment compared to vehicle (1.1 ± 0.4-fold). The levels of iNC were diminished to undetectable levels in the PBMC of both the ASC and SVF treatment grou compared to the vehicle group (1.8 ± 0.3-fold; Fig. 6B).

Serum was isolated from the peripheral blood of all of the mice 10 days after treatment to detect the persistence of inflammatory mediators in circulation. Of all of the detected mediators, the greatest change occurred in the levels of the anti-inflammatory cytokine IL-1 following ASC (0.025 NAR) and SVF (0.027 NAR) treatment, compared to the vehicle control group (0.015 NAR). While the levels of TNF-α were measurable in the serum of vehicle-treate (0.007 NAR) and ASC-treated (0.008 NAR EAE) mice, TNF-α was undetectable in the SVF-treat EAE mice sera. Similarly, a large reduction in IFN-γ was seen in the sera of SVF-treated (0.00 NAR) EAE mice compared to the sera of vehicle-treated (0.012 NAR) and ASC-treated (0.011 NAR) EAE mice. No differences were detected in the levels of IL-1α between the vehicle, ASC, and SVF treatment groups with values of 0.022 NAR, 0.021 NAR, and 0.023 NAR, respectively The vehicle control (0.246 NAR) and SVF treatment (0.231 NAR) groups had comparable leve of G-CSF levels, while higher levels were measure in the ASC treatment group (0.344 NAR; Fi 7).

Discussion

Both ASC and SVF treatment improved the severity of disease, behavior, and motor functior EAE mice after pathologic impairment. The data from this study correlate the therapeutic effects induced by ASC or SVF at late-stage disease. In the EAE model, the CNS is the site of immune-mediated pathologic degeneration. To provide a more comprehensive understand of the mechanisms that facilitated these improvements, evaluation of the peripheral blood and lymphoid tissues was also performed to investigate the immunomodulatory and anti-inflammatory outcomes. Robust modulation of inflammation markedly improved neurodegeneration with either ASC or SVF treatments as demonstrated by improvements to CNS pathology and the partial recovery of motor function. Interestingly, analysis of the peripheral tissues revealed potent effects following SVF treatment. Key shifts in the frequencies and phenotypes of several types of immune cells were evaluated in the lympho tissues and peripheral blood, which suggests that SVF produced a novel immunomodulatory capacity compared to ASC. SVF mediated alterations to the immune cells and associated factors in the periphery that consistently suggested enhancement of anti-inflammatory and regulatory cell phenotypes concomitant to diminished pathogenic effector cell responses.

The data indicate that SVF treatment promoted an anti-inflammatory milieu in the CNS that may support regenerative processes that resulted in functional improvements. Together, th marked enhancement of IL-10 expressions in the CNS and peripheral tissues with the consistent increased frequencies of helper T cells, B cells, and macrophages suggest import modulation toward favorable phenotypes, thus altered function, pertinent to the mechanisr

mediated encephalitogenic features in EAE 28, 29. During autoimmune and chronic inflammatory diseases including EAE and MS, tolerance is lost and effector T cells cause pathology 2, 4, 29. By promoting the beneficial helper T cell subtype, the regulatory T cells (Tregs), and associated IL-10 production is a therapeutic mechanism vital for the maintenan and restoration of immune tolerance 30, 31. Our study demonstrated that SVF treatment enhanced the helper T cell populations in all examined peripheral tissues that correlated wi high levels of TGF-β and IL-10 which indicate induction of Tregs. Additionally, $CD4^+$ $CD25^+$ $foxp3^+$ Tregs were detected in the lymph nodes 10 days following SVF treatment. The differential regulation of T cell subsets by alteration of the cytokine repertoire within the loc environment is integral to the resulting immune responses 32, 33. Although considered pro inflammatory by production of IFN-γ, the differentiation of Th1 cells can suppress Th17 cells 29. Likewise, differentiation of Th2 and Tregs suppress Th17 cell responses 2, 14. Consistent with the analysis of the spleens, SVF treatment enhanced cytokine expressions associated w Th1, Th2, and Tregs and diminished Th17 responses. Our data indicate that treatment with S promoted immunomodulatory effects that countered the autoimmune and inflammatory responses and promoted immune tolerance. This evidence is consistent with the outcomes other preclinical and clinical studies using stem cell-based therapies to treat EAE 31, 34, 35, 36-38, and other autoimmune, inflammatory diseases 14, 15, 39, 40.

Macrophage phenotypes can also be skewed according to the disease milieu and cytokine repertoires. The classical activation macrophages, formerly known as the M1 type, are predominant during inflammatory stimuli, produce iNOS, and mediate tissue damage. On th contrary, the alternative activation macrophages, or M2 type, constitutively express Arg-1 ar are attributed to anti-inflammatory effects and wound healing 41-43. High levels of IL-10 car induce the alternative activation macrophages, and in turn produce more IL-10 and TGF-β, which has been shown to ameliorate disease in models of MS 44, 45. Along with the high lev of IL-10 and TGF-β following SVF treatment, the marked increases in macrophage frequencie in the peripheral blood, lymph nodes, and spleen suggest that the alternative activation macrophages were preferentially promoted. Moreover, the concomitant high expression of Arg-1 detected in the spleens and PBMC with the diminished iNOS expression in the lymph nodes and PBMC strongly suggest mechanisms involving macrophages that ameliorate disease by SVF therapy.

Further investigation into the mechanisms that SVF treatment directly modulate immune ce are underway to better understand the effects of SVF therapy. These findings further suppo the potent immunomodulatory effects of SVF therapy during autoimmune and chronic inflammatory disease milieus in EAE. For the translational implications, most MS patients

demonstrates the use of SVF as a promising therapeutic candidate for MS patients in a clinically relevant scenario. Furthermore, SVF in currently used in clinical settings for reconstructive procedures and is isolated by rapid automated methods after liposuction. Th proposed use of SVF cells is perhaps a better alternative to culture expanded ASC with regar to eliminating the need for good manufacturing practice-level cell processing laboratories 4(

Conclusion

SVF treatment robustly and comprehensively ameliorated pre-existing neurodegeneration i the EAE mouse model of MS. The therapeutic effects of SVF resulted in improvements to motor function, CNS tissues, and alterations in the peripheral lymphoid tissues and blood. T date, this is the first investigation elucidating the global effects of SVF treatment at late-stag disease in the EAE model.

Acknowledgments

Much appreciation to Dina Gaupp of the histology core and Alan Tucker of the flow cytomet core for their valuable technical contributions, and the veterinary and vivarium staff of the Tulane University Department of Comparative Medicine.

Author Contributions

A.C.B.: Conception and design, provision of study material, collection and/or assembly of da data analysis and interpretation, manuscript writing; A.L.S.: Conception and design, provisio of study material, collection and/or assembly of data, data analysis and interpretation; R.M.\ R.C.T., B.Y.G., M.F.D., and R.S.H.: Collection and/or assembly of data, data analysis and interpretation; J.M.G.: Administrative support, manuscript writing; B.A.B.: Conception and design, financial support, administrative support, provision of study material, manuscript writing, final approval of manuscript.

Disclosure of Potential Conflicts of Interest

The authors indicate no potential conflicts of interest. Dr. Gimble is a co-owner and Chief Scientific Officer of LaCell LLC, a for profit biotechnology company focusing on preclinical an clinical research involving adipose derived stem cells. The commercial affiliation with LaCell, LLC does not alter the adherence to any policies on sharing data and materials.

References

Citing Literature

STEM CELLS
STEM CELLS Translational Medicine
The Oncologist